The mouse HP1 proteins are essential for preventing liver tumorigenesis

Nehmé Saksouk[1-4*], Shefqet Hajdari[1-4*], Marine Pratlong[5], Célia Barrachina[5], Céline Graber[6], Aliki Zavoriti[1-4], Amélie Sarrazin[6], Nelly Pirot[1-4], Jean-Yohan Noël[1-4], Lakhdar Khellaf[4], Eric Fabbrizio[1-4, 7], Eric Julien[1-4, 7], Florence M. Cammas[1-4, 7]

[1] IRCM, Institut de Recherche en Cancérologie de Montpellier, Montpellier, F-34298, France.

[2] INSERM, U1194, Montpellier, F-34298, France.

[3] Université de Montpellier, Montpellier, F-34090, France.

[4] Institut régional du Cancer de Montpellier, Montpellier, F-34298, France.

[5] MGX, Biocampus Montpellier, CNRS, INSERM, Univ Montpellier, Montpellier, France

[6] IGBMC, Institut de Génétique, de Biologie Moléculaire et Cellulaire, Illkirch, France

[7] MRI, BioCampus Montpellier, CNRS, INSERM, Univ Montpellier, Montpellier, France

[8] CNRS, Route de Mende, Montpellier, France

Corresponding author: Florence Cammas, Florence.cammas@inserm.fr

* Contributed equally to the work

Abstract

Chromatin organization is essential for appropriate interpretation of the genetic information. Here, we demonstrated that the chromatin associated proteins HP1 are dispensable for cell survival but are essential within hepatocytes to prevent liver tumor development. Molecular characterization of pre-malignant HP1-Triple KO livers revealed that HP1 are required for maintenance of the H3K9me3 and H4K20me3 heterochromatin marks but not for overall genome stability nor for the expression of major satellites. HP1-TKO livers are also characterized by inappropriate expression of many genes involved in crucial liver functions such as regulation of the redox and endoplasmic reticulum equilibrium, lipid metabolism and steroid biosynthesis. Finally, we showed that some of these genes were over-expressed through the reactivation of specific endogenous retrovirus, most likely through the inactivation of the KRAB-ZFP/TRIM28 axis. Our findings indicate that HP1 proteins act as guardians of liver homeostasis to prevent tumor development through the modulation of multiple chromatin-associated events.

Keywords: chromatin; HP1; cancer; liver; transcriptional silencing; endogenous retrovirus; oxidative stress

Introduction

Chromatin dynamic organization is essential for the interpretation of genetic information in a cell-type and tissue-specific manner (Prakash and Fournier, 2018). Alteration of this organization can have devastating consequences, as evidenced by the large number of diseases induced by mutations in chromatin-associated proteins (Koschmann et al., 2017; Mirabella et al., 2016), as well as by the dramatic changes in chromatin organization observed in cancer cells (Mai, 2018). Although extensively studied in the past three decades, it is still largely unknown how chromatin organization is regulated and involved in whole organism homeostasis.

Chromatin can be divided according to its structural and functional features in euchromatin and heterochromatin. Euchromatin displays low level of compaction, is highly enriched in genes, and is transcriptionally competent. Conversely heterochromatin is highly compacted, enriched in repetitive DNA sequences, and mostly silent. Although, heterochromatin was considered for a long time as an inert compartment with the single function of silencing parasite DNA sequences, it is now recognized as a dynamic and functional compartment (Janssen et al., 2018a). Heterochromatin Protein 1 (HP1) proteins were first isolated as major heterochromatin components in *Drosophila* (James and Elgin, 1986). These proteins are highly conserved from yeast to mammals which express three isoforms (HP1α, HP1β and HP1γ) that are distributed in both eu- and heterochromatin. These proteins are characterized by a N-terminal chromodomain (CD), which is involved in the recognition of the heterochromatin-associated histone marks H3 lysine-9 di- or trimethylated (H3K9me2/3), and a C-terminal chromoshadow domain (CSD), which, through dimerization, constitutes a platform for interaction with many protein partners. These two domains are separated by the hinge domain that is crucial for HP1 association with RNA and recruitment to heterochromatin (Eissenberg and Elgin, 2014; Lomberk et al., 2006). Thus, HP1 proteins, through this structural organization, are at the crossroads of the structural and functional organization of chromatin. Accordingly, HP1 are important for heterochromatin

65 silencing, chromosome segregation, regulation of gene expression, DNA repair and DNA
66 replication (Dinant and Luijsterburg, 2009; Fanti and Pimpinelli, 2008; Nishibuchi and
67 Nakayama, 2014). Functionally, HP1 proteins are essential for embryonic development in
68 several organisms, including *Drosophila* (Eissenberg et al., 1992), C. *elegans* (Schott et al.,
69 2006) and the mouse (our unpublished data). HP1α is essential for the plasticity of T helper
70 (Th2) lymphocytes (Allan et al., 2012), HP1β for neuro-muscular junctions (Aucott et al.,
71 2008) and HP1γ for spermatogenesis (Abe et al., 2011; Brown et al., 2010). Several studies
72 also suggested a correlation between the level of HP1 expression and cancer development
73 and/or metastasis; however, how HP1 are involved in these processes remains largely to be
74 clarified (Dialynas et al., 2008; Vad-Nielsen and Nielsen, 2015).

75 Liver chromatin organization has been well characterized in several physio-
76 pathological conditions (Janssen et al., 2018b). In addition, several known HP1 partners,
77 including the transcription cofactors TRIM24 and TRIM28, and the histone-lysine N-
78 methyltransferase SUV39H1, play key roles in hepatocytes. Therefore, hepatocytes
79 constitute an excellent model to investigate HP1 roles in chromatin functions (Bojkowska et
80 al., 2012a; Fan et al., 2013; Hardy and Mann, 2016; Herquel et al., 2011; Khetchoumian et
81 al., 2007). We therefore decided to inactivate all HP1 encoding genes specifically in mouse
82 hepatocytes (HP1-TKO mice). Unexpectedly, we found that HP1-TKO hepatocytes can
83 survive and contribute to liver functions throughout life but HP1-TKO animals developed liver
84 tumors at old age. Coupled with our molecular analysis, these data highlighted a new
85 function of HP1 proteins as guardians of liver homeostasis through the modulation of various
86 chromatin-associated events including maintenance of heterochromatin organization,
87 regulation of gene expression and silencing of specific ERV.

88

89

RESULTS

HP1 proteins are dispensable for hepatocyte proliferation and survival

To unravel HP1 *in vivo* functions, the HP1β and HP1γ encoding-genes (*Cbx1* and *Cbx3,* respectively) were inactivated in the liver of HP1αKO mice (Allan et al., 2012) using the Cre recombinase expressed under the control of the hepatocyte-specific albumin promoter (Postic et al., 1999; Weisend et al., 2009) (Fig. 1A). Liver-specific excision of the *Cbx1* and *Cbx3* alleles was confirmed by PCR (Fig. 1B), and the level of HP1β and HP1γ protein expression was checked by western blotting. At 7 weeks post-partum as well as at middle-aged (3-6 months), the overall level of HP1β and HP1γ was decreased by about 60% in mutant as compared to controls livers (Fig. 1C). Furthermore, immuno-fluorescence (IF) analysis of liver cryo-sections using anti-HP1β and -HP1γ antibodies showed that their expression was lost in about 60% of liver cells in mutant mice compared with controls (Fig. 1D). As this percentage is similar to the estimated 60-70% hepatocyte fraction within liver, these findings indicated that both proteins were concomitantly depleted in most hepatocytes (Si-Tayeb et al., 2010). As expected since *Cbx5* (HP1α-encoding gene) was knocked out in all body cells, HP1α could not be detected in mutant livers (Fig. 1B-C). These animals were thereafter called HP1-triple knockout (HP1-TKO). Histological analysis of hematoxylin/eosin/Safran (HES) stained paraffin-embedded liver sections from 7-week-old (young) and 3-6-month-old (middle-aged) control and HP1-TKO animals did not reveal any significant alteration of the structural organization of hepatocytes nor of the liver parenchyma (Supplementary Figure 1). In agreement with this observation, analysis of proliferation (Ki67) and apoptosis (Activated caspase 3) by immuno-histochemistry (IHC) of Tissue Micro Arrays (TMA) containing liver sections from young and middle-aged control and HP1-TKO mice did not reveal any significant difference between mutant and control animals (Fig. 1E1-2). As HP1 have been shown to play critical roles in genome stability (Bosch-Presegué et al., 2017; Shi et al., 2008), IHC was also performed with an antibody against the phosphorylated form

of H2AX (γH2AX), a marker of DNA damage (Kuo and Yang, 2008). The number of γH2AX-positive cells was not significantly different in livers from young and middle-aged HP1-TKO and control animals, suggesting that HP1 proteins depletion did not lead to major genomic instability within hepatocytes (Fig. 1E3).

To unambiguously test the viability of hepatic cells in absence of any HP1 isoform, we established bipotential hepatic BMEL (Bipotential Mouse Embryonic Liver) cell lines according to the protocol described by Strick-Marchand & Weiss (Strick-Marchand and Weiss, 2002) inactivated for all HP1 encoding genes as illustrated on figure 1F. As assessed by western blotting, none of the HP1 were expressed in these cells that were thereafter called HP1-TKO (Fig. 1G). These cells were morphologically similar to control cells and had a tendency to proliferate faster than control cells (Fig. 1H). Altogether, these data demonstrated that in mouse, the three HP1 proteins are dispensable for hepatocyte survival both *in vivo* and *ex vivo* as well as for the appropriate structural organization of the liver parenchyma throughout life.

Heterochromatin organization is altered in HP1-TKO hepatocytes

Since, HP1 are well-known components of chromatin, we assessed the impact of their loss on chromatin sub-nuclear organization and functions in liver and BMEL cells. First, the level of different heterochromatin-associated histone marks was investigated by western blotting. H3K9me3 and H4K20me3, two marks of constitutive heterochromatin, were strongly decreased in the liver of 7-week-old and middle-aged HP1-TKO mice compared with age-matched controls. Conversely, no change of H3K27me3, a facultative heterochromatin mark, nor of H3K9me2, H4K20me2 and H4K20me1 was observed in these same samples (Fig. 2A). The decrease of H3K9me3 without any significant change of H3K27me3 nor of H3K4me3 was also observed in HP1-TKO as compared to control BMEL cells (Fig. 2B). IF analysis indicated that the high level of H3K9me3 associated with chromocenters (i.e., DAPI-dense structures that contain structural components of heterochromatin) observed in control

BMEL cells was drastically reduced in HP1-TKO cells, whereas the labeling within euchromatin was not significantly affected (Fig. 2C). The level and distribution of methylated DNA was assessed by IF using an antibody against 5-methyl cytosine (5mC). This analysis showed no difference between control and HP1-TKO BMEL cells (Fig. 2C). Although these results suggested that the absence of the three HP1 proteins affected heterochromatin organization, chromocenters still clustered, but tended to be more associated with the nuclear periphery in HP1-TKO hepatocytes than in control cells (Fig. 2D1). To more precisely quantify the distribution of chromocenters, nuclei were divided in four co-centric areas in which the intensity of DAPI staining was measured using the cell profiler software (schema in Fig. 2D2). In control nuclei, DAPI staining was roughly homogeneously distributed throughout the four areas (Fig. 2D2). Conversely, in HP1-TKO nuclei, DAPI intensity increased progressively from the inner part to the external part. This indicated that in the simultaneous absence of all HP1 isoforms, heterochromatin tended to be more associated with the nuclear periphery than in control nuclei. This was not associated with any significant change of the level nor distribution of laminB1 (LamB1) as assessed by IF, strongly suggesting that although the level of heterochromatin is reduced at the nuclear periphery, the absence of HP1 did not lead to any significant alteration of the nuclear envelop organization (Fig.2C). We then measured the expression and the number of major satellite repeats that represent the main component of pericentromeric heterochromatin. Surprisingly this analysis revealed no significant alteration and even a tendency of these repeats to be down-regulated in absence of HP1 in both liver and BMEL cells whereas the number of these repeats within the genome was unchanged (Fig. 2E and data not shown). These data demonstrated that in hepatocytes, although HP1 proteins are essential for the maintenance of constitutive heterochromatin-associated histone marks and for the sub-nuclear organization of chromocenters, they are not required for the regulation of major satellite expression nor for their stability.

HP1 proteins are involved in the regulation of liver-specific gene expression programs

To investigate the effect of the loss HP1 on gene expression, an unbiased RNA-seq transcriptomic analysis was performed on libraries prepared from 7 week-old control and HP1-TKO liver RNA. This analysis showed that 1215 genes were differentially expressed between control and HP1-TKO liver samples (with a 1.5-fold threshold difference and an adjusted $P \leq 0.05$) (Fig. 3A). As expected on the basis of the established role of HP1 as gene silencers in several cellular and animal models and of the loss of the repressive H3K9me3 mark (this study), more genes were up-regulated (730) than down-regulated (485) in HP1-TKO compared with control livers (Supplementary Table 1). These genes were distributed throughout the genome without preferential chromosomal location, compared with the global gene distribution (Supplementary Figure 2).

Analysis of differentially expressed genes (HP1-dependent genes) using David Gene Ontology (https://david.ncifcrf.gov/) and Gene Set Enrichment Analysis (GSEA; http://software.broadinstitute.org/gsea/index.jsp) programs revealed that several biological processes were significantly affected in HP1-TKO livers. The most striking feature of this analysis was the very high enrichment of genes encoding for the Krüppel Associated Box (KRAB) domain within up-regulated genes (P = 5.8E-26) (Fig. 3B & Supplementary Tables 1 & 2). The up-regulation of several of these genes (*Rsl1*, *Zfp345*, *Zfp445* and *Zkscan3*) was validated by RT-qPCR in 7-week-old HP1-TKO livers compared with age-matched controls (Fig. 3C). Beside these KRAB domain encoding genes, up-regulated genes were also enriched in genes classified as belonging to the GO terms signal peptide, immunity, guanylate-binding protein, response to virus, etc... (Fig. 3B), strongly suggesting activation of an inflammatory response in HP1-TKO livers (Fig. 3B-C & Supplementary Table 4). Genes encoding for members of the p450 cytochrome (CYP) family were also strongly enriched in HP1-dependent genes with 7 up-regulated and 18 down-regulated amongst the 79 CYP genes detected in the present RNAseq analysis. Mammalian P450s are membrane bound

mostly in the endoplasmic reticulum (ER) and some in the mitochondria and play essential roles within liver (Guengerich, 2018). These genes are involved in numerous metabolic processes including reduction-oxidation (redox) processes, steroid hormone biosynthesis and lipid metabolic process (Bhattacharyya et al., 2014; Park et al., 2014). In particular, 11 HP1-dependent genes encode for members of the CYP2 family involved in ER and redox functions (Table 1). Moreover, *Nox4*, the gene encoding the nicotinamide adenine dinucleotide phosphate (NADPH) oxidase isoform most consistently associated with ER and ROS in liver (Paik et al., 2014), was significantly down-regulated in HP1-TKO as compared with control livers (Fig. 3C & Supplementary Table 1). It was thus not surprising that oxidation-reduction, ER, steroid hormone biosynthesis, lipid metabolic process were amongst the most affected functions in HP1-TKO livers (Fig. 3B & Supplementary Tables 2; 3; 5 and 6). The differential expression of several genes involved in liver-specific functions such as *Cyp2c29* and *Cyp2b10* (ER and redox), *Ifit2* (interferon γ signature) and *Nox4* (ROS production) was validated by RT-qPCR in 7 week-old HP1-TKO and age-matched control livers (Fig. 3C).

These data demonstrated that although the liver of HP1-TKO animals did not display any significant phenotypical abnormality, HP1 proteins are required for regulating directly or indirectly the expression of several genes with key functions for liver homeostasis.

The loss of HP1 leads to reactivation of specific endogenous retroviruses and up-regulation of associated genes

As mentioned above genes encoding for the KRAB domain were highly enriched in up-regulated genes in HP1-TKO livers. The KRAB domain is almost exclusively present in the KRAB-Zinc Finger Protein (KRAB-ZFP) family of transcriptional repressors (Yang et al., 2017). The best characterized genomic target of these repressors are themselves through an auto-regulatory loop and retrotransposons of the endogenous retroviruses (ERV) family

(O'Geen et al., 2007; Yang et al., 2017). The expression of DNA repeats was therefore investigated in our RNA-seq dataset. To this end, the coordinates of all annotated DNA repeats of the RepeatMasker database (mm10 assembly) were aligned against the RNA-seq reads and only those that could be assigned unambiguously to a specific genomic locus were analyzed. In total, 846 repeats were deregulated in HP1-TKO livers compared with control livers: 603 (71.3%) were up-regulated and 243 (28.7%) down-regulated (Fig. 4A & Supplementary Table 7). Among the most represented up-regulated repeats, 59.4% were ERV, 19.2% long interspersed nuclear elements (LINEs) and 9.3% short interspersed elements (SINEs) whereas the genome-wide distribution of these elements was 26.8% ERVs, 45.1% LINEs and 17.3% SINEs (Fig. 4B & Supplementary Table 7). This biased distribution of repetitive elements strongly supported the hypothesis that HP1 proteins were preferentially involved in ERV silencing.

To determine whether the differential expression of such repeats in HP1-TKO livers could be associated with deregulation of gene expression, we first generated a map of HP1-dependent repeats located in the vicinity of HP1-dependent genes. To this end, 100kb were added on both sides of each HP1-dependent gene, and the HP1-dependent repeats present in these regions were scored. This analysis showed that a fraction of HP1-dependent genes (138 up-regulated and 94 down-regulated) was associated with HP1-dependent repeats. Interestingly, this physical association between HP1-dependent repeats and HP1-dependent genes correlated with a functional association since 84% of repeats associated with up-regulated genes were also up-regulated and 75.5% of repeats associated with down-regulated genes were down-regulated (Fig. 4C & Supplementary Tables 8 & 9). Analysis of the distance between HP1-dependent genes and HP1-dependent repeats showed that up-regulated repeats tended to be located closer to up-regulated genes rather than to down-regulated genes, whereas inversely down-regulated repeats tended to be located closer to down than up-regulated genes. As a control, the alignment of all annotated repeats against HP1-dependent genes showed that repeats were homogeneously distributed in the regions

surrounding both up-regulated and down-regulated genes (Fig. 4D). Altogether, this analysis strongly suggested a link between the loss of HP1, the reactivation of some ERV and the up-regulation of genes in their neighborhood. In agreement with this conclusion, several deregulated genes associated with deregulated repeats such as *Mbd1*, *Bglap3*, *Obpa*, *Bmyc*, *Fbxw19* and *Zfp445* have already been shown to be controlled by ERVs (Fig. 4E; Ecco et al. 2016; Herquel et al. 2013). Interestingly, *Zfp445* was associated with four up-regulated MERK26-int repeats that were at nearly equal distance between this gene and *Zkscan7,* another KRAB-ZFP-encoding gene also up-regulated in HP1-TKO liver. This suggested that the reactivation of these specific repeats might interfere with the expression of both genes (Fig. 4E).

Altogether, these data strongly suggested that the HP1-dependent expression of specific genes rooted in the HP1-dependent reactivation of certain repeats, mainly of the ERV family, within the genome. Whether these repetitive regulatory elements are used in physiological conditions remains to be studied. These results could seem paradoxical with the increased expression of several KRAB-ZFPs that are known to be involved in ERV silencing; however, they are in agreement with the proposed mechanism of auto-regulation of KRAB-ZFP-encoding genes through interaction with the corepressor TRIM28 (O'Geen et al., 2007). We therefore hypothesized that in HP1-TKO livers, KRAB-ZPF-encoding genes and their targets including ERVs are over-expressed because of a HP1-dependent loss of TRIM28 activity.

HP1 is necessary for TRIM28 activity within liver

To investigate the relationship between HP1, KRAB-ZFPs, TRIM28 and ERVs in liver, RNA-seq, RT-qPCR and western blot assays were used to analyze the effect of HP1 loss on TRIM28 expression in liver. Neither TRIM28 mRNA nor protein expression were significantly altered in HP1-TKO as compared to control livers demonstrating that HP1 were not required for the regulation of TRIM28 expression but rather for its activity (Fig. 5A-B). To assess whether the loss of association between TRIM28 and HP1 could recapitulate the phenotype

induced by the loss of HP1 on TRIM28 functions, we used the previously described mouse models in which either a mutated TRIM28 protein that cannot interact with HP1 (T28HP1box) is expressed instead of the WT TRIM28 protein or in which TRIM28 is depleted (T28KO) specifically within liver (Herquel et al., 2011; Herzog et al., 2011). As expected, western-blot analysis indicated that TRIM28 expression was strongly decreased in T28KO livers, whereas it was only decreased by about two-fold in T28HP1box livers (this mutation is present only on one *Trim28* allele, and the other one is inactivated) (Fig. 5C). The level of the three HP1 proteins was not affected in these mouse strains. RT-qPCR analysis showed that several HP1-dependent genes including *Nox4*; *Cypc29* and *Rsl1* were not affected in T28HP1box and T28KO livers (Fig. 5D). Conversely, *Cyp2b10; Ifit2* and the KRAB-ZFP-encoding genes *Zfp345* and *Zfp445* that were all over-expressed in HP1-TKO liver were also up-regulated in T28HP1box and T28KO livers (Fig. 5D). The higher expression level of *Ifit2* and *Zfp345* in T28HP1box as compared to T28KO livers strongly suggested a dominant negative role of T28HP1box on their expression. Altogether, these data demonstrated that HP1 proteins regulate gene expression through TRIM28-dependent and -independent mechanisms. To test whether the HP1-dependent ERV-associated genes also required TRIM28, the expression of *Mbd1* and *Bglap3* was assessed in T28KO and T28HP1box livers. Like in HP1-TKO livers, they were over-expressed in both T28KO and T28HP1box livers, although to a lesser extent as compared to HP1-TKO livers suggesting that HP1 were able to partially repress the expression of these two genes even in the absence of TRIM28 (Fig. 5E).

HP1 proteins prevent tumor development in liver

Analysis of old mice (>44 weeks of age) showed that although HP1-TKO animals were morphologically indistinguishable from control littermates, 72.7% of females (n=11) and 87.5% of males (n=8) had developed liver tumors whereas none of the female (n=24) and 9.1% of male (n=44) controls did so (Fig. 6A). The number and size of tumors were very

304 variable among animals (Fig. 6B), suggesting that the absence of HP1 generated an
305 environment prompt to tumorigenesis and that other factors were also involved in this
306 process. Analysis of the excision of the floxed *Cbx*1 (HP1β) and *Cbx*3 (HP1γ) genes showed
307 equivalent rate of recombination in both the tumor and healthy liver tissues indicating that
308 tumors originated from HP1-TKO hepatocytes (Supplementary Fig. 3A). Histological analysis
309 of paraffin-embedded liver tissue sections revealed that most old male (M-TKO) and female
310 (F-TKO) HP1-TKO animals developed tumor nodules that could easily be distinguished from
311 the rest of the liver parenchyma (Fig. 6C). These nodules were characterized by the
312 presence of well-differentiated hepatocytes but without their specific trabecular organization,
313 and thus, were identified as typical hepatocellular carcinoma (HCC). Moreover, RT-qPCR
314 analysis of the expression of α-fetoprotein (*Afp*), a marker of human HCC, in control and in
315 normal (TKON) and tumor (TKOT) HP1-TKO liver samples showed that *Afp* was strongly
316 over-expressed exclusively in the tumor tissue of three of the five tested tumors
317 (Supplementary Figure 3C). Analysis of cell proliferation (Ki67), apoptosis (activated caspase
318 3) and global response to DNA damage (γH2AX) by IHC on TMA of paraffin-embedded liver
319 sections from old mice showed a two-fold increase of cell proliferation in both the tumor
320 (TKOT) and non-tumor (TKON) parts of HP1-TKO liver samples compared with control parts
321 whereas no change was detected in the number of apoptotic-positive cells nor of positive
322 γH2AX cells (Supplementary Fig. 3B).

323 Similarly, T28KO and T28HP1box mice older than 42 weeks of age developed more
324 frequently tumors in livers than controls, although at a lower rate than HP1-TKO animals
325 (38.5% and 35.7% for T28KO and T28HP1box males and 26.3% and 31.2% for T28KO and
326 T28HP1box females, respectively, Fig. 6D-E) strengthening the mechanistic link between
327 HP1 proteins and TRIM28 for liver tumor prevention.

328 Finally, analysis of the expression of the ERV-associated genes *Mbd1* and *Bglap3* in old
329 animals (Fig. 6F) showed that both genes were up-regulated in both normal (TKON) and
330 tumor (TKOT) liver parts from old HP1-TKO animals as compared to control livers. In

331 contrast, *Mbd1* was no longer over-expressed in the liver (normal and tumor parts) of old
332 TRIM28 mutant mice. For *Bglap3*, a slight over-expression was observed in T28KO but not in
333 T28HP1box old animals, and in both cases the level of expression was very low as
334 compared to HP1-TKO mice (Fig. 6G). These data showed that HP1 were required to
335 maintain repression of the *Mbd1* and *Bglap3* genes most likely through the silencing of the
336 associated ERV throughout life and that this function was mostly independent of TRIM28 in
337 old animals.

338

DISCUSSION

In this study, we used the Cre-LoxP system to inactivate the three chromatin-associated HP1 proteins specifically within hepatocytes as soon as they acquired their identity during mouse development (Weisend et al., 2009). We demonstrated that the loss of HP1 proteins lead to the loss of the heterochromatin marks H3K9me3 and H4K20me3 and to the over-expression of specific retrotransposons but surprisingly not of the major satellite repeats. Furthermore, we demonstrated that HP1 are not required for cell viability but are critical within hepatocytes for preventing liver tumor development.

The finding that in the mouse, HP1 proteins were not essential for neither cell viability nor liver function was in contrast with many studies showing the fundamental functions of each HP1 isoform in various pluripotent and differentiated cellular systems (Huang et al., 2017; Mattout et al., 2015) as well as during embryonic development in various species, such as *Drosophila* (Eissenberg et al., 1992), C. *elegans* (Schott et al., 2006) and the mouse (our unpublished data). One can hypothesize that liver chromatin organization and functions are highly specific and mostly independent of HP1 and/or that some compensatory mechanisms through yet unknown factors, take place specifically in mouse liver (Eissenberg and Elgin, 2014; Kwon and Workman, 2011; Nishibuchi and Nakayama, 2014). In favor of the hypothesis of a specific liver chromatin organization, it is important to note that liver is mostly quiescent throughout life but is able to regenerate upon stress (e.g., partial hepatectomy) essentially through the re-entry of quiescent and fully differentiated hepatocytes into cell cycle rather than via stem cell proliferation, like in other tissues (Fausto et al., 2006; Kurinna and Barton, 2011). This specific ability of differentiated hepatocytes to enter/exit quiescence could rely on a peculiar loose chromatin organization that might be less sensitive to the loss of HP1 as compared to other cell types. To this respect, it is interesting to note that liver is the tissue that express the lowest level of all HP1 isoforms (https://www.proteinatlas.org).

We showed that HP1 loss was accompanied by a drastic reduction of the two heterochromatin marks H3K9me3 and H4K20me3 and a partial re-localization of DAPI-dense structures towards the nucleus periphery. However, in contrast to the results reported upon loss of H3K9me3 induced by inactivation of the histone methyltransferases SUV39H1 and SUV39H2, the loss of H3K9me3 in HP1-TKO hepatocytes did not result in neither decrease of H3K9me2 nor over-expression of major satellite repeats, but rather in their slight down-regulation (Lehnertz et al., 2003; Velazquez Camacho et al., 2017). This observation supports the conclusion that HP1 are essential to maintain H3K9me3 but not H3K9me2 throughout life and that this latter histone modification is sufficient to keep major satellite sequences at a low level of transcription. It has been reported that SUV39H1 over-expression is associated with HCC development (Fan et al., 2013) and that HCC induced by a methyl-free diet is also characterized by elevated SUV39H1 expression and increased H3K9me3 but with reduced H4K20me3 deposition (Pogribny et al., 2006). This suggests that decreased level of H4K20me3 rather than of H3K9me3 in HP1-TKO mice could be a key determinant of tumorigenesis. In support of this hypothesis, H4K20me3 has been reported to be essential for genome integrity that is known to be essential for cell identity and for proper timing of heterochromatin replication whose deregulation has recently been proposed to be involved in cancers (Brustel et al., 2017; Du et al., 2019; Jørgensen et al., 2013). Further investigations are required to determine which, if any, alteration of heterochromatin organization induced by the lack of the three HP1 proteins is involved in tumorigenesis.

HP1 ablation also led to the deregulation (both up- and down-regulation) of many genes, strongly suggesting that the three HP1 proteins are involved in both repression and activation of gene expression, as reported by others (Eissenberg and Elgin, 2014; Lee et al., 2013; Piacentini et al., 2009; Vakoc et al., 2005). Many of these genes are involved in liver specific functions and it will be interesting to identify the determinant for their responsiveness to HP1 depletion. Of particular interest, we found that many genes encoding for the p450 cytochrome family (Cyp) were deregulated in HP1 mutant mice. Several of these proteins are

391 involved in the detoxification of the liver and in oxidative stress that are two key factors in
392 hepatocarcinogenesis (Takaki and Yamamoto, 2015). How these genes are regulated by
393 HP1 remains to be determined, however nuclear receptors of the Peroxisome Proliferation-
394 Activated Receptors (PPAR) have been shown to be important in this process (Cizkova et
395 al., 2012). Interestingly, we found that PPARγ was strongly down-regulated in HP1 mutant
396 mice and it is tempting to speculate that this low expression of PPARγ underlies the
397 deregulation of several *Cyp* genes. Furthermore, HP1-TKO livers were also characterized by
398 a transcriptional signature of an interferon γ response strongly suggesting liver inflammation,
399 another well-recognized factor for hepatocarcinogenesis. What is the leading cause of
400 inflammation in HP1 mutant mice is still unknown but might be link to a continuum moderate
401 cellular dysfunction induced by the altered transcriptome in these mice. Finally, one of the
402 most striking result in the present study was the enrichment in genes encoding members of
403 the KRAB-ZFP family of transcriptional co-repressors. The KRAB domain is almost
404 exclusively present in the KRAB-Zinc Finger Protein (KRAB-ZFP) family of transcriptional
405 repressors that have the particularity to be still actively evolving in mammals (Yang et al.,
406 2017). Little information is available about the functions of most of these transcription factors,
407 however it is now well recognized that transposable elements of the ERV family are one of
408 their main targets through the recruitment of the TRIM28 corepressor (Jacobs et al., 2014;
409 Wolf et al., 2015; Yang et al., 2017). These mobile genetic elements constitute a threat for
410 the genome stability and/or gene expression because of their ability to insert at any genomic
411 location. Thus, an important challenge for the genome is to keep all these elements silent
412 and unable to get transposed. However and paradoxically, increasing evidence suggests that
413 they have been co-opted to serve as regulatory sequences in the host genome (Thompson
414 et al., 2016). Here, we found that, although HP1 proteins were shown to be dispensable for
415 ERV silencing in ES cells (Maksakova et al., 2011), they are involved in silencing of specific
416 ERVs in liver. We provide evidence that this function relies on the inactivation of the KRAB-
417 ZFP/TRIM28 complex. Although we have not yet identified the determinants underlying the
418 HP1-dependency of specific retrotransposons, our data strongly suggest that the reactivation

of some ERVs induce the over-expression of genes in their vicinity. Some of these ERVs, as those associated the *Zfp445*, *Fbwx19* and *Obp2a* genes, behave either as enhancer-like elements as proposed by others (Bojkowska et al., 2012b; Herquel et al., 2013), whereas others rather behave as alternative promoters (e.g., for the *Mbd1* and *Bglap3* genes). Interestingly, inactivation of the nuclear receptor corepressor TRIM24 leads to *Mbd1, Zfp445, Obp2a* over-expression, whereas inactivation of the KRAB-ZFP corepressor TRIM28 causes over-expression of *Bglap3 and Fbxw19* (Ecco et al., 2016; Herquel et al., 2013). Altogether, these data strongly suggest that HP1 acts upstream of these two corepressors, a conclusion in line with our previous observation that TRIM24 and TRIM28 can be found in the same complex in liver (Herquel et al., 2011), and with our hypothesis that HP1 regulates TRIM28 activity in liver. Because the depletion of either of these two corepressors also lead to HCC and because the over-expression of ERV has been proposed to play a role in tumorigenesis (Scarfò et al., 2016), we propose that one mechanism by which HP1 prevent tumor development is by silencing specific ERVs.

Although we cannot conclude yet about the exact mechanisms underlying HP1 functions in preventing tumor development, our study highlighted major HP1 roles in heterochromatin organization, regulation of gene expression and ERV silencing the alteration of which, as discussed above, could all contribute to hepatocyte transformation and liver tumorigenesis.

MATERIALS AND METHODS

Mouse models.

The Cbx5KO, T28KO (TRIM28KO) and T28HP1box (TRIM28-L2/HP1box) mouse strains were described previously (Allan et al., 2012; Cammas et al., 2000; Herzog et al., 2011). Exons 2 to 4 within the *Cbx1* gene (HP1β), and exon 3 within the *Cbx3* gene (HP1γ) were surrounded by LoxP sites. Excision of the floxed exons exclusively in hepatocytes by using mice that express the Cre recombinase under the control of the albumin promoter (Alb-Cre mice, (Postic et al., 1999)) led to the removal of the starting ATG codon of the two genes, as well as to a frameshift within the CSD-encoding sequence of *Cbx1* and the CD-encoding sequence of *Cbx3. Cbx5,* the gene encoding HP1α, was inactivated in all body cells by removing exon 3 using the Cre recombinase under the control of the cytomegalovirus (CMV) promoter, as described previously (Cbx5KO mice) (Allan et al., 2012). *Cbx5*+/- animals were then crossed with *Cbx3*L2/L2 and Cbx1L2/L2 animals to generate mice in which all three proteins can be depleted in tissues upon expression of the Cre recombinase. *Cbx5*+/-; *Cbx3*L2/L2; Cbx1L2/L2 were crossed with Alb-Cre transgenic mice to produce *Cbx5*+/-; *Cbx3*L2/+; Cbx1L2/+; Alb-Cre mice that were intercrossed to finally produce HP1-TKO mice and their controls. TRIM28L2/HP1box were crossed with Alb-Cre transgenic mice to produce mice that express TRIM28HP1box as the only TRIM28 protein in hepatocytes (TRIM28-liverL-/HP1box, called T28HP1box mice in this article).

For each experiment, experimental and control mice were age-matched and whenever possible were littermates. A minimum of three animals of each genotype were used for each experiment. This number was deemed sufficiently appropriate to account for normal variation, as determined from previous studies. The number of animals used for each experiment is indicated in the figure legends. No statistical method was used to predetermine sample size.

Mice were housed in a pathogen-free barrier facility, and experiments were approved by the national ethics committee for animal warfare (n°CEEA-36).

Antibodies/oligonucleotides

The antibodies used in this study were: the rabbit anti-TRIM28 polyclonal antibody PF64, raised against amino acids 141–155 of TRIM28[64]; the anti-HP1α, anti-HP1β and anti-HP1γ monoclonal antibodies 2HP2G9, 1MOD1A9, and 2MOD1G6[65], respectively. Anti-Casp3A (9661, Cell Signaling); anti-γH2AX (Ab11174, Abcam), anti-Ki67 (M3064, Spring Bioscience). Anti-5mC (NA81, Calbiochem). Oligonucleotides are described in Supplementary Table 10.

Tissue processing for histology.

For fresh frozen tissues, 3mm sections of the liver large lobe were embedded in the OCT compound (TissueTek) following standard protocols, and 18μm-thick sections were cut using a Leica CM1850 cryostat and stored at −80 °C.

For paraffin-embedded tissues, 3mm sections of the liver large lobe were fixed in 4% neutral-buffered formalin (VWR Chemicals) at room temperature (RT) overnight, and stored in 70% ethanol at 4°C. Fixed tissues were processed using standard protocols and embedded in paraffin wax. Three-µm-thick sections were cut using a Thermo Scientific Microm HM325 microtome, dried at 37 °C overnight and stored at 4 °C.

Immuno-fluorescence analysis.

Cryo-sections were fixed in formaldehyde (2%) at RT for 15min, and then air dried at RT for 20min. Sections were rinsed in PBS (3 x 15min) and incubated in 5% BSA/PBS/0.3% Triton X-100 at RT for 30min to block non-specific antibody binding. Sections were the incubated with primary antibodies diluted in 1% BSA/PBS/0.3% Triton X-100 at 4 °C overnight, or at RT for 1 h. Sections were then washed in PBS/0.1% Triton X-100 (3 × 5 min) and incubated with the appropriate secondary antibody [goat-anti-rabbit Alexa Fluor 488 (Molecular Probes, 1:800), goat-anti-mouse Alexa Fluor 568 (Molecular Probes, 1:800)] diluted in 1% BSA/PBS/0.3% Triton X-100 at RT for 1h. After three washes (5min/each) in PBS/0.1% Triton X-100, sections were washed in water for 5 min before mounting with VECTASHIELD

mounting medium (Vector Laboratories) with 4',6-Diamidino-2-Phenylindole, Dihydrochloride (DAPI). Sections were dried at RT overnight, and then kept at 4°C before image acquisition with a Zeiss Apotome2 microscope and analysis using ImageJ.

Immuno-histochemistry.

Paraffin-embedded liver sections were processed for routine hematoxylin, eosin and Safran or reticulin staining. For immuno-histochemistry, sections were washed in PBS/1% Triton X-100 at RT (3 x 30 min) and incubated in blocking solution (PBS/1% Triton X-100/10% fetal calf serum/0.2% sodium azide) at RT twice for 1h, followed by incubation in 3% H_2O_2 in blocking solution at 4 °C overnight. This was followed by two washes of 15 min/each in blocking solution, and incubation with primary antibodies at 4 °C overnight. Sections were washed in blocking solution (3 x 1h), and then in PBS/1% Triton X-100 (3 x 10min). The secondary antibody was diluted in blocking solution (without sodium azide) and added at RT for 1h. Sections were then washed in PBS (3 × 1 h) before mounting with VECTASHIELD mounting medium with DAPI. Images were acquired with a Zeiss Apotome2 microscope and processed using ImageJ.

RNA extraction and RT-qPCR assays

RNA was isolated from liver samples using TRIzol, according to the manufacturer's recommendations (Life technologies). 2µg of total RNA was incubated with 2U of DNase 1 at 37°C for 30min. For reverse transcription, a mixture containing 2µg of DNA-free total RNA, 0.125µg of random primers and 0.25µg of oligodT was denatured at 70°C for 10min, and then incubated with 1U Superscript III (Invitrogen) at 50°C for 1h. 1/100 of this reaction was used for real-time qPCR amplification using SYBR Green I (SYBR Green SuperMix, Quanta).

RNA-seq

Total RNA from liver samples from 7-week-old control and HP1-KO mice was used for library preparation using the Illumina TruSeq Stranded mRNA Sample Preparation kit.

Polyadenylated RNA was purified using magnetic oligo(dT) beads and then fragmented into small pieces using divalent cations at elevated temperature. The cleaved RNA fragments were copied into first-strand cDNA using reverse transcriptase and random primers in the presence of actinomycin D. Second-strand cDNA synthesis was performed using dUTP, instead of dTTP, resulting in blunt double-stranded cDNA fragments. A single 'A' nucleotide was added to the 3' ends of the blunt DNA fragments using a Klenow fragment (3' to 5'exo minus). The cDNA fragments were ligated to double-stranded TruSeq Universal adapters using T4 DNA Ligase. The ligated products were enriched by PCR amplification (98°C for 30sec, followed by 15 cycles of 98°C for 10sec, 60°C for 30sec, and 72°C for 30sec; finally, 72°C for 5min). Then, the excess of PCR primers was removed by purification using AMPure XP beads (Agencourt Biosciences Corporation). The quality and quantity of the final cDNA libraries were checked using a Fragment Analyzer (AATI) and the KAPA Library Quantification Kit (Roche), respectively. Libraries were equimolarly pooled and sequenced (50nt single read per lane) on a Hiseq2500 apparatus, according to the manufacturer's instructions. Image analysis and base calling were performed using the Illumina HiSeq Control software and the Illumina RTA software. Reads not mapping to rRNA sequences were mapped onto the mouse genome mm10 assembly using the Tophat mapper (v2.0.10 58) and the Bowtie2 (v2.1.0) aligner. Gene expression was quantified from uniquely aligned reads using HTSeq v0.5.4p3 59 and gene annotations from the Ensembl release 75.

Statistical analyses were performed using the method previously described (Love et al., 2014) implemented in the DESeq2 Bioconductor library (v1.0.19), taking into account the batch effect. Adjustment for multiple testing was performed with the Hochberg and Benjamini method (Hochberg and Benjamini, 1990).

For repeat analysis, alignment positions were compared with repeats annotated in UCSC with RepeatMasker (rmsk table from mm10) and overlaps were kept relative to the strand. Among the multiple mapped reads, only those mapping to the same repeat type were kept. Repeat types that were significantly different between conditions were identified with

DESeq2 v1.0.19. Repeats found in exons were removed from the analysis because it was not possible to discriminate between differential gene and repeat expression.

Data are available at GEO (accession number: GSE119244).

Extraction of mouse liver nuclei

Adult male mice were euthanized, and their livers removed and placed on ice. After dissection of the liver lobes and removal of the connective tissue and blood vessels, approximately 100 µg of liver tissue was washed in ice-cold homogenizing buffer (HB, 0.32M sucrose, 5mM $MgCl_2$, 60mM KCl, 15mM NaCl, 0.1mM EGTA, 15mM Tris-HCl pH 7.4), minced with scissors, and homogenized with 7 ml of HB using a 15 ml Wheaton Dounce homogenizer and 20 strokes of the loose B pestle. Unless otherwise indicated, all subsequent steps were performed at 4°C. Homogenates were filtered through 100 µM layers of gauze, taken to 7 ml with HB and centrifuged in 15 ml Corning tubes at 6000 g for 10min. After discarding the supernatant, pellets were gently resuspended in the same tube with 2 ml of HB and 2 ml of nuclear extraction buffer (HB plus 0.4% Nonidet P-40) and incubated on ice for 10min. The mixtures were centrifuged (10.000 g for 10 min) in two tubes in which 8ml of separating buffer (1.2M sucrose, 5mM $MgCl_2$, 60mM KCl, 15mM NaCl, 0.1mM EGTA, 15mM Tris-HCl pH 7.4) was added. Pellets were resuspended in 1.0 ml of 0.25M sucrose and 1mM $MgCl_2$, and transferred to a 1.5 ml Eppendorf tube. Nuclei were collected by centrifugation at 700 g at 4 °C for 10 min and stored at -70°C until use.

Statistics and reproducibility.

The Microsoft Excel software was used for statistical analyses; the used statistical tests, number of independent experiments, and P-values are listed in the individual figure legends. All experiments were repeated at least twice unless otherwise stated.

ACKNOWLEDGMENTS:

We thank P. Chambon, C. Sardet, T. Forné, D.Fisher, E. Julien and C. Grimaud for helpful discussions and critical reading of the manuscript. We thank F. Bernex and L. LeCam, C. Keime and B. Jost for fruitful discussions. We thank L. Papon, H. Fontaine and C. Bonhomme for technical assistance and M. Oulad-Abdelghani and the IGBMC for the anti-HP1 and TRIM28 antibodies. We also thank the RHEM technical facility and particularly J. Simony for histological analysis and the IGBMC/ICS transgenic and animal facility for the initial establishment of the HP1 and TRIM28 mouse models. We thank C. Vincent and the IRCM animal core facility for the day to day care of the animal models. Finally, we thank S. Chamroeun for counting positive cells on TMA. We acknowledge the imaging facility MRI, member of the national infrastructure France-BioImaging and supported by the French National Research Agency (ANR-10-INBS-04, «Investments for the future»).

This work was supported by funds from the Centre National de la Recherche Scientifique (CNRS), the Institut National de la Santé et de la Recherche Médicale (INSERM), the University of Montpellier and the Institut regional de Cancérologie de Montpellier (ICM). SH was funded by an Erasmus PhD fellowship. We also thank the Ministry of Education, Science and Technology of the Republic of Kosovo for a scholarships to support SH. FC was supported by grants from ANR (ANR 2009 BLAN 021 91; ANR-16CE15-0018-03), INCa (PLBIO13-146), ARC (PJA20131200357), and La ligue Régionale contre le Cancer (128-R13021FF-RAB13006FFA). Sequencing was performed by the MGX facility. Montpellier, France.

AUTHORS' CONTRIBUTIONS:

NS and SH performed the analysis of mice and interpreted the data. MP and CB made the libraries, generated and analyzed the RNA-seq data. AZ performed most of the RT-qPCR experiments. NP supervised the histological core facility and JYN performed the TMA. LK performed the pathological analysis of histological sections. EF performed some of the RT-qPCR analyses. EJ interpreted the data. FC designed, analyzed and interpreted the data and wrote the manuscript with input from all co-authors.

DECLARATION OF INTEREST: No competing interests

FIGURES:

Figure 1: **HP1are not required for hepatocyte survival nor for liver organization and function**. (A) Schematic representation of the strategy to inactivate the three HP1-encoding genes (*Cbx1*, *3* and *5*) specifically in hepatocytes using the recombinase Cre expressed under the control of the albumin promoter. For details see *Materials & Methods* section. (B) The hepatocyte-specific excision (L- alleles) of the *Cbx1* (HP1β) and *Cbx3* (HP1γ) genes and ubiquitous excision of *Cbx5* (HP1α) in HP1-TKO (1-4) mice was verified by PCR. Controls were littermates with either L2 (*Cbx*1 and *Cbx*3) or "+" (*Cbx*5) alleles (5-8). Note that control #7 is $Cbx5^{L-/+}$. (C) Western blot analysis of whole-cell extracts from liver samples confirmed the absence of HP1α and the decreased expression of HP1β and HP1γ, due to the hepatocytes-specific excision of the corresponding genes in HP1-TKO as compared to age-matched control mice. Ponceau staining was used as loading control. (D) Immuno-fluorescence analysis of liver tissue cryosections confirmed the absence of HP1β and HP1γ expression in about 60% of cells in 7-weeks old HP1-TKO mice compared with controls. (E1-3). (G) Immuno-histochemistry analysis of paraffin-embedded liver sections revealed no significant difference in proliferation (Ki67), apoptosis (caspase 3A), and DNA damage (γH2AX) between HP1-TKO (n=5 7-week-old and n= 5 3-6month-old mice) and control mice (n=7 7-week- and n= 4 3-6-month-old mice). The number of positive cells were normalized to the total number of cells in each section and graphs recapitulating these data are shown as the mean ± SEM. ns, no significant difference (Student's t-test). (F) Schematic representation of the strategy to establish BMEL cells from *Cbx5*-/-; *Cbx1*L2/L2; *Cbx3*L2/L2 fetal livers and to inactivate the three HP1-encoding genes. (G) Western blot analysis of whole-cell extracts

from BMEL cells confirmed the absence of all HP1 isoforms in HP1-TKO (*Cbx5*-/-; *Cbx1*L2/L2, *Cbx3*L2/L2; Cre-ERT treated with tamoxifen). "Het" were *Cbx5*+/-; *Cbx1*L2/L2 BMEL cells and "Ctl" were *Cbx5*-/-; *Cbx1*L2/L2; *Cbx3*L2/L2; Cre-ERT non treated with tamoxifen. (H) Proliferation curves of "Het", 2 Ctl clones (C3 and C5) and 2 HP1-TKO clones (KO1 and KO3). The graph represent the average of three independent experiments done in triplicates.

Figure 2: **HP1 are essential for heterochromatin organization but not to regulate the expression of major satellites**. (A) HP1 are essential for the maintenance of the two heterochromatin hallmarks H3K9me3 and H4K20me3 in hepatocytes. Western blot analysis of nuclear extracts from liver of 7-week-old and middle-aged (3-6-month-old) controls (Ctl: 1; 2; 5; 6) and HP1-TKO (TKO: 3; 4; 7; 8) mice with antibodies against the indicated histone marks. Ponceau staining was used as loading control. (B) HP1 are also essential for the maintenance of the H3K9me3 in BMEL cells. (C) IF analysis showed that H3K9me3 is lost on pericentromeric heterochromatin foci of HP1-TKO (TKO) BMEL cells without significant change in the distribution of H3K27me3. (D1-2) Loss of HP1 leads to a partial relocation of DAPI-dense regions (arrows) towards the nuclear periphery. Representative images of paraffin-embedded liver tissue sections from 7-week-old control (Ctl) and HP1-TKO (TKO) mice stained with DAPI (63x magnification). To select mostly hepatocytes, only the largest nuclei with a size comprised between 70 and 150 μm^2 and with a circular shape were selected for this analysis. 2D sections of nuclei were divided in four concentric areas (1 to 4) and DAPI staining intensity was quantified using the cell profiler software. The mean fractional intensity at a given radius was calculated as the fraction of the total intensity normalized to the fraction of pixels at a given radius in n=584 control and n=762 HP1-TKO (TKO) nuclei. Data are the mean ± SEM. ***p value <0.001. (E) Loss of the three HP1 proteins in hepatocytes does not affect the expression of major satellites. qPCR assays were performed using total RNA from livers of 7-week-old control (n=4) and HP1-TKO mice (n=4) and on control (Ctl) and HP1-TKO (TKO) BMEL.

Figure 3: **HP1 are essential regulators of gene expression in liver**. (A) MA plot after DSeq2 normalization of RNA-seq data from 7-week-old control (n=3) and HP1-TKO (n=4) liver RNA samples. Red dots represent genes that are differentially expressed between controls and HP1-TKO mice (adjusted p-value p <0.05). (B) Functional analysis of the differentially expressed genes using the DAVID Gene Ontology software. (C) Validation by RT-qPCR of the altered expression of the indicated genes. RNA was extracted from livers of 7-weeks Controls (n=4) and HP1-TKO (n=4) animals. Data were normalized to *Hprt*

664 expression and are shown as the mean ± SEM. ns, no significant difference *p value <0.05;
665 ***p value <0.001 (Student's t-test).

666 **Figure 4**: **HP1 are required for silencing specific endogenous retroviruses (ERVs) in**
667 **hepatocytes.** (A) MA-plot after DSeq2 normalization of RNA-seq reads including repeats
668 aligned against the Repbase database. Red dots represent genes and repeats that are
669 differentially expressed between controls and HP1-TKO liver samples (p<0.05). (B) ERVs are
670 over-represented in repeats that are up-regulated upon loss of all HP1 isoforms (Repeat_Up)
671 compared to repeats that are down-regulated (Repeat_Down) and to the genome-wide
672 distribution of repeats according to the RepeatMasker database (All). (C) Repeats over-
673 expressed in HP1-TKO liver samples compared with controls (Repeat_Up) are over-
674 represented in regions (± 100kb) around genes that are over-expressed in HP1-TKO
675 (genes_up). Conversely, repeats down-regulated in HP1-TKO liver samples compared with
676 controls (Repeat_Down) are over-represented in regions (± 100kb) around genes repressed
677 in HP1-TKO (genes_down). (D) Repeats that are up-regulated or down-regulated upon HP1
678 protein loss tend to be closer to genes that are up- or down-regulated in HP1-TKO,
679 respectively. The absolute distance (in base pairs) was measured from the gene
680 transcriptional start site and from the beginning of the repeat, according to the RepeatMasker
681 annotation. (E) Representative Integrative Genomic Viewer snapshots of the indicated up-
682 regulated genes associated with up-regulated repeat sequences.

683

684 **Figure 5**: **HP1 proteins are involved in the recruitment and/or maintenance of TRIM28**
685 **at chromatin in hepatocytes.** (A) TRIM28 expression is independent of HP1 proteins. RT-
686 qPCR quantification of TRIM28 expression in total RNA from livers of 7-week-old control (Ctl;
687 n=4) and HP1-TKO (TKO; n=4) mice. Data were normalized to *Hprt* expression and are
688 shown as the mean ± SEM. (B) Western blot analysis of 50µg of whole cell extracts from
689 livers of 7-week-old control (1 and 2) and HP1-TKO (3 to 5) mice using an anti-TRIM28
690 polyclonal antibody. Tubulin was used as loading control. (C) The loss of interaction between
691 TRIM28 and HP1 proteins does not significantly alter the level of expression of TRIM28 and
692 of the HP1 proteins. 50 µg of whole liver extracts from 7-week-old controls (n=2), T28KO
693 (n=3) and T28HP1box (n=3) mice were analyzed by western blotting using the anti-TRIM28
694 polyclonal antibody and anti-HP1α, β and γ monoclonal antibodies. GAPDH and Ponceau
695 staining were used as loading controls. (D) TRIM28 is involved in the regulation of the
696 expression of some but not all HP1-dependent genes. RT-qPCR analysis using liver RNA
697 samples from 5 week-old control (n=5), T28KO (n=5) and T28HP1box (n=5) mice. Data were
698 normalized to *Hprt* expression and are shown as the mean ± SEM. (E) TRIM28 is involved in

699 the regulated expression of HP1- and ERV-dependent genes. Expression of *Mbd1* and
700 *Bglap3* by RT-qPCR analysis using liver RNA samples from 7-week-old control (Ctl) and
701 HP1-TKO (TKO) mice, and 5-week-old control (n=5), T28KO (n=5) and T28HP1box (n=5)
702 mice. Data were normalized to *Hprt* expression and are shown as the mean ± SEM. ns, no
703 significant difference *p value <0.05; ***p value <0.001 (Student's t-test).

704 **Figure 6**: **HP1 and their association with TRIM28 prevent tumor development in liver.**
705 (A) Controls (n=67) and HP1-TKO (TKO, n=17) animals older than one year of age were
706 sacrificed and the percentage of animals with tumors (morphological and histological
707 analysis) was calculated. (B) Morphology of the livers with tumors (arrows) in three HP1-TKO
708 females (F TKO1, 2 and 3) and three HP1-TKO males (M TKO1, 2 and 3) older than one
709 year of age. The liver morphology of one age-matched control female and male is also
710 shown (F Ctl and M Ctl, respectively). (C) Liver histological analysis (hematoxylin-eosin-
711 Safran staining) of one representative HP1-TKO female (F-TKO) and one representative
712 HP1-TKO male (M-TKO). If it is one the livers shown in (B) I would add the number (ex. M
713 TKO1). Upper panels: tumor/liver parenchyma interface highlighted by arrowheads (low
714 magnifications). Bottom panels: magnification (x 100) of the boxes in the upper panels
715 showing the tumor in the right part of the images (thick plates of atypical hepatocytes). A
716 venous tumor thrombus is also present (asterisk). Need higher magnifications or better
717 photos because it is difficult to see anything. (D) The association between TRIM28 and
718 HP1 α, β and γ is essential in hepatocytes to prevent liver tumor development. Control
719 (n=42), T28KO (n=32) and T28HP1box (n=30) mice older than one year of age were
720 sacrificed and the percentage of animals with tumors (morphological and histological
721 analysis) was calculated. (E) Liver histological analysis (hematoxylin-eosin-Safran staining)
722 of representative animals. (F) The expression of *Bglap3* and *Mbd1* was higher also in livers
723 from old (>1year old) HP1-TKO mice. RT-qPCR analysis was performed using RNA from old
724 control (n=7), and HP1-TKO liver samples (TKON for normal part, TKOT for tumor part)
725 (n=7). (G) The alteration of *Mbd1* and *Bglap3* expression upon loss of the association
726 between TRIM28 and HP1 proteins was not maintained in old animals. RT-qPCR analysis
727 using RNA from control (n=5), T28KO (T28KON for normal part, T28KOT for tumor part)
728 (n=5) and T28HP1box (T28HP1boxN for normal part, T28HP1boxT for tumor part) livers
729 (n=5). Data were normalized to *Hprt* expression and are shown as the mean ± SEM. ns, no
730 significant difference *p value <0.05; **p value <0.01; ***p value <0.001 (Student's t-test).

731

732

TABLES:

Table 1: HP1-dependent p450 genes.

Gene name	Log2 fold-change	padj	Redox	Endoplasmic reticulum	Drug metabolism	Lipid metabolism	Steroid synthesis
Cyp2b10	4.06	1.41E-38	1	1	0	0	1
Cyp2b9	2.68	4.51E-10	1	1	0	0	1
Cyp2b13	1.80	0.000120	0	0	0	0	1
Cyp4f16	1.63	1.36E-09	0	0	0	0	0
Cyp2d12	1.38	0.000468	0	0	0	0	1
Cyp2a4	1.09	0.0342	0	0	0	0	0
Cyp2a22	1.06	0.000559	0	0	0	0	0
Cyp2f2	-0.65	0.00318	1	1	0	0	0
Cyp4f13	-0.67	0.0151	0	0	0	0	0
Cyp2r1	-0.72	0.0173	1	1	0	0	0
Cyp27a1	-0.83	1.30E-05	1	0	0	0	0
Cyp2d37-ps	-0.83	0.0319	0	0	0	0	0
Cyp3a25	-0.85	0.00222	1	1	0	0	1
Cyp39a1	-0.88	0.00164	1	1	0	1	0
Cyp2e1	-0.94	7.81E-05	1	1	1	0	1
Cyp2d26	-0.95	2.57E-05	1	1	0	0	1
Cyp2a5	-0.97	0.00129	0	0	0	0	0
Cyp2d13	-1.00	0.00445	0	0	0	0	0
Cyp1a2	-1.25	3.65E-12	1	1	1	1	1
Cyp2c53-ps	-1.31	0.01178	0	0	0	0	0
Cyp2d40	-1.42	6.83E-06	0	0	0	0	1
Cyp46a1	-1.64	0.000629	1	1	0	1	0
Cyp3a59	-2.15	3.62E-17	1	0	0	0	0
Cyp2c44	-2.20	2.18E-20	0	0	0	0	1
Cyp2c29	-2.60	7.65E-25	1	1	0	0	1

(1) found and (0) not found according to the David Gene Ontology software.

SUPPLEMENTARY INFORMATIONS:

Supplementary Figure 1: HP1 are not required for liver structural organization. The absence of HP1 proteins in hepatocytes did not induce any significant histological alteration in the liver of young (7-week-old) and middle-aged (3-6-month-old) HP1-TKO mice. (A-D) low magnification, (E-H) high magnification.

Supplementary Figure 2: Genome-wide distribution of HP1-dependent genes. The distribution of HP1-dependent genes (up and down) was compared with all genes (genome) and genes detected in our RNA-seq analysis (RNA-seq).

Supplementary Figure 3: HP1-TKO tumors originate from hepatocytes lacking HP1. (A) Excision of the *Cbx1* and *Cbx3* genes in the liver of old (x-week-old) HP1-TKO mice (TKON: normal part of liver; TKOT: tumor part of liver) compared with age-matched controls (CTL). (B) Expression of the α-fetoprotein (*Afp*) gene in the liver of old control (CTL) and HP1-TKO mice. (C) Quantification of Ki67-, caspase 3A- and γH2AX-positive cells on liver Tissue Micro Areas of old HP1-TKO mice and age-matched controls.

Supplementary table 1: analysis of RNAseq data comparing control and HP1-TKO liver total RNA

Supplementary table 2: functional clustering of genes up-regulated upon loss of HP1 witin hepatocytes (https://david.ncifcrf.gov/)

Supplementary table 3: functional clustering of genes down-regulated upon loss of HP1 witin hepatocytes (https://david.ncifcrf.gov/)

Supplementary table 4: HP1-dependent genes belonging to the IFNγ response pathway

Supplementary table 5: HP1-dependent genes with liver specific functions

Supplementary table 6: genes with liver-specific expression according to the Tissue Specific Gene Expression and Regulation software (bioinfo.wilmer.jhu.edu/tiger)

Supplementary table 7: Fold change of HP1-dependent repeats

Supplementary table 8: repeats with increased expression upon loss of HP1 associated with genes up-regulated upon loss of HP1

Supplementary table 9: repeats with decreased expression upon loss of HP1 associated with genes down-regulated upon loss of HP1

768 **Supplementary table 10: list of the oligonucleotides used in this study**

769

770

771 **REFERENCES**

772

773 Abe, K., Naruse, C., Kato, T., Nishiuchi, T., Saitou, M., and Asano, M. (2011). Loss of heterochromatin
774 protein 1 gamma reduces the number of primordial germ cells via impaired cell cycle progression in
775 mice. Biol. Reprod. *85*, 1013–1024.

776 Allan, R.S., Zueva, E., Cammas, F., Schreiber, H.A., Masson, V., Belz, G.T., Roche, D., Maison, C., Quivy,
777 J.-P., Almouzni, G., et al. (2012). An epigenetic silencing pathway controlling T helper 2 cell lineage
778 commitment. Nature *487*, 249–253.

779 Aucott, R., Bullwinkel, J., Yu, Y., Shi, W., Billur, M., Brown, J.P., Menzel, U., Kioussis, D., Wang, G.,
780 Reisert, I., et al. (2008). HP1-beta is required for development of the cerebral neocortex and
781 neuromuscular junctions. J. Cell Biol. *183*, 597–606.

782 Bhattacharyya, S., Sinha, K., and Sil, P.C. (2014). Cytochrome P450s: mechanisms and biological
783 implications in drug metabolism and its interaction with oxidative stress. Curr. Drug Metab. *15*, 719–
784 742.

785 Bojkowska, K., Aloisio, F., Cassano, M., Kapopoulou, A., Santoni de Sio, F., Zangger, N., Offner, S.,
786 Cartoni, C., Thomas, C., Quenneville, S., et al. (2012a). Liver-specific ablation of Krüppel-associated
787 box-associated protein 1 in mice leads to male-predominant hepatosteatosis and development of
788 liver adenoma. Hepatology *56*, 1279–1290.

789 Bojkowska, K., Aloisio, F., Cassano, M., Kapopoulou, A., Santoni de Sio, F., Zangger, N., Offner, S.,
790 Cartoni, C., Thomas, C., Quenneville, S., et al. (2012b). Liver-specific ablation of Krüppel-associated
791 box-associated protein 1 in mice leads to male-predominant hepatosteatosis and development of
792 liver adenoma. Hepatology *56*, 1279–1290.

793 Bosch-Presegué, L., Raurell-Vila, H., Thackray, J.K., González, J., Casal, C., Kane-Goldsmith, N., Vizoso,
794 M., Brown, J.P., Gómez, A., Ausió, J., et al. (2017). Mammalian HP1 Isoforms Have Specific Roles in
795 Heterochromatin Structure and Organization. Cell Rep *21*, 2048–2057.

796 Brown, J.P., Bullwinkel, J., Baron-Lühr, B., Billur, M., Schneider, P., Winking, H., and Singh, P.B. (2010).
797 HP1gamma function is required for male germ cell survival and spermatogenesis. Epigenetics
798 Chromatin *3*, 9.

799 Brustel, J., Kirstein, N., Izard, F., Grimaud, C., Prorok, P., Cayrou, C., Schotta, G., Abdelsamie, A.F.,
800 Déjardin, J., Méchali, M., et al. (2017). Histone H4K20 tri-methylation at late-firing origins ensures
801 timely heterochromatin replication. EMBO J. *36*, 2726–2741.

802 Cammas, F., Mark, M., Dollé, P., Dierich, A., Chambon, P., and Losson, R. (2000). Mice lacking the
803 transcriptional corepressor TIF1beta are defective in early postimplantation development.
804 Development *127*, 2955–2963.

805 Cizkova, K., Konieczna, A., Erdosova, B., Lichnovska, R., and Ehrmann, J. (2012). Peroxisome
806 Proliferator-Activated Receptors in Regulation of Cytochromes P450: New Way to Overcome
807 Multidrug Resistance? J Biomed Biotechnol *2012*.

808 Dialynas, G.K., Vitalini, M.W., and Wallrath, L.L. (2008). Linking Heterochromatin Protein 1 (HP1) to
809 cancer progression. Mutat. Res. *647*, 13–20.

Dinant, C., and Luijsterburg, M.S. (2009). The emerging role of HP1 in the DNA damage response. Mol. Cell. Biol. *29*, 6335–6340.

Du, Q., Bert, S.A., Armstrong, N.J., Caldon, C.E., Song, J.Z., Nair, S.S., Gould, C.M., Luu, P.-L., Peters, T., Khoury, A., et al. (2019). Replication timing and epigenome remodelling are associated with the nature of chromosomal rearrangements in cancer. Nat Commun *10*, 416.

Ecco, G., Cassano, M., Kauzlaric, A., Duc, J., Coluccio, A., Offner, S., Imbeault, M., Rowe, H.M., Turelli, P., and Trono, D. (2016). Transposable Elements and Their KRAB-ZFP Controllers Regulate Gene Expression in Adult Tissues. Dev. Cell *36*, 611–623.

Eissenberg, J.C., and Elgin, S.C.R. (2014). HP1a: a structural chromosomal protein regulating transcription. Trends Genet. *30*, 103–110.

Eissenberg, J.C., Morris, G.D., Reuter, G., and Hartnett, T. (1992). The heterochromatin-associated protein HP-1 is an essential protein in Drosophila with dosage-dependent effects on position-effect variegation. Genetics *131*, 345–352.

Fan, D.N.-Y., Tsang, F.H.-C., Tam, A.H.-K., Au, S.L.-K., Wong, C.C.-L., Wei, L., Lee, J.M.-F., He, X., Ng, I.O.-L., and Wong, C.-M. (2013). Histone lysine methyltransferase, suppressor of variegation 3-9 homolog 1, promotes hepatocellular carcinoma progression and is negatively regulated by microRNA-125b. Hepatology *57*, 637–647.

Fanti, L., and Pimpinelli, S. (2008). HP1: a functionally multifaceted protein. Curr. Opin. Genet. Dev. *18*, 169–174.

Fausto, N., Campbell, J.S., and Riehle, K.J. (2006). Liver regeneration. Hepatology *43*, S45-53.

Guengerich, F.P. (2018). Cytochrome P450 research and The Journal of Biological Chemistry. J. Biol. Chem.

Hardy, T., and Mann, D.A. (2016). Epigenetics in liver disease: from biology to therapeutics. Gut *65*, 1895–1905.

Herquel, B., Ouararhni, K., Khetchoumian, K., Ignat, M., Teletin, M., Mark, M., Béchade, G., Van Dorsselaer, A., Sanglier-Cianférani, S., Hamiche, A., et al. (2011). Transcription cofactors TRIM24, TRIM28, and TRIM33 associate to form regulatory complexes that suppress murine hepatocellular carcinoma. Proc. Natl. Acad. Sci. U.S.A. *108*, 8212–8217.

Herquel, B., Ouararhni, K., Martianov, I., Le Gras, S., Ye, T., Keime, C., Lerouge, T., Jost, B., Cammas, F., Losson, R., et al. (2013). Trim24-repressed VL30 retrotransposons regulate gene expression by producing noncoding RNA. Nat. Struct. Mol. Biol. *20*, 339–346.

Herzog, M., Wendling, O., Guillou, F., Chambon, P., Mark, M., Losson, R., and Cammas, F. (2011). TIF1β association with HP1 is essential for post-gastrulation development, but not for Sertoli cell functions during spermatogenesis. Dev. Biol. *350*, 548–558.

Hochberg, Y., and Benjamini, Y. (1990). More powerful procedures for multiple significance testing. Stat Med *9*, 811–818.

Huang, C., Su, T., Xue, Y., Cheng, C., Lay, F.D., McKee, R.A., Li, M., Vashisht, A., Wohlschlegel, J., Novitch, B.G., et al. (2017). Cbx3 maintains lineage specificity during neural differentiation. Genes Dev. *31*, 241–246.

849 Jacobs, F.M.J., Greenberg, D., Nguyen, N., Haeussler, M., Ewing, A.D., Katzman, S., Paten, B., Salama,
850 S.R., and Haussler, D. (2014). An evolutionary arms race between KRAB zinc-finger genes ZNF91/93
851 and SVA/L1 retrotransposons. Nature *516*, 242–245.

852 James, T.C., and Elgin, S.C. (1986). Identification of a nonhistone chromosomal protein associated
853 with heterochromatin in Drosophila melanogaster and its gene. Mol. Cell. Biol. *6*, 3862–3872.

854 Janssen, A., Colmenares, S.U., and Karpen, G.H. (2018a). Heterochromatin: Guardian of the Genome.
855 Annu. Rev. Cell Dev. Biol.

856 Janssen, A., Colmenares, S.U., and Karpen, G.H. (2018b). Heterochromatin: Guardian of the Genome.
857 Annu. Rev. Cell Dev. Biol.

858 Jørgensen, S., Schotta, G., and Sørensen, C.S. (2013). Histone H4 lysine 20 methylation: key player in
859 epigenetic regulation of genomic integrity. Nucleic Acids Res. *41*, 2797–2806.

860 Khetchoumian, K., Teletin, M., Tisserand, J., Mark, M., Herquel, B., Ignat, M., Zucman-Rossi, J.,
861 Cammas, F., Lerouge, T., Thibault, C., et al. (2007). Loss of Trim24 (Tif1alpha) gene function confers
862 oncogenic activity to retinoic acid receptor alpha. Nat. Genet. *39*, 1500–1506.

863 Koschmann, C., Nunez, F.J., Mendez, F., Brosnan-Cashman, J.A., Meeker, A.K., Lowenstein, P.R., and
864 Castro, M.G. (2017). Mutated Chromatin Regulatory Factors as Tumor Drivers in Cancer. Cancer Res.
865 *77*, 227–233.

866 Kuo, L.J., and Yang, L.-X. (2008). Gamma-H2AX - a novel biomarker for DNA double-strand breaks. In
867 Vivo *22*, 305–309.

868 Kurinna, S., and Barton, M.C. (2011). Cascades of transcription regulation during liver regeneration.
869 Int. J. Biochem. Cell Biol. *43*, 189–197.

870 Kwon, S.H., and Workman, J.L. (2011). The changing faces of HP1: From heterochromatin formation
871 and gene silencing to euchromatic gene expression: HP1 acts as a positive regulator of transcription.
872 Bioessays *33*, 280–289.

873 Lee, D.H., Li, Y., Shin, D.-H., Yi, S.A., Bang, S.-Y., Park, E.K., Han, J.-W., and Kwon, S.H. (2013). DNA
874 microarray profiling of genes differentially regulated by three heterochromatin protein 1 (HP1)
875 homologs in Drosophila. Biochem. Biophys. Res. Commun. *434*, 820–828.

876 Lehnertz, B., Ueda, Y., Derijck, A.A.H.A., Braunschweig, U., Perez-Burgos, L., Kubicek, S., Chen, T., Li,
877 E., Jenuwein, T., and Peters, A.H.F.M. (2003). Suv39h-mediated histone H3 lysine 9 methylation
878 directs DNA methylation to major satellite repeats at pericentric heterochromatin. Curr. Biol. *13*,
879 1192–1200.

880 Lomberk, G., Wallrath, L., and Urrutia, R. (2006). The Heterochromatin Protein 1 family. Genome Biol.
881 *7*, 228.

882 Love, M.I., Huber, W., and Anders, S. (2014). Moderated estimation of fold change and dispersion for
883 RNA-seq data with DESeq2. Genome Biol. *15*, 550.

884 Mai, S. (2018). The 3D Cancer Nucleus. Genes Chromosomes Cancer.

885 Maksakova, I.A., Goyal, P., Bullwinkel, J., Brown, J.P., Bilenky, M., Mager, D.L., Singh, P.B., and
886 Lorincz, M.C. (2011). H3K9me3-binding proteins are dispensable for SETDB1/H3K9me3-dependent
887 retroviral silencing. Epigenetics Chromatin *4*, 12.

888 Mattout, A., Aaronson, Y., Sailaja, B.S., Raghu Ram, E.V., Harikumar, A., Mallm, J.-P., Sim, K.H.,
889 Nissim-Rafinia, M., Supper, E., Singh, P.B., et al. (2015). Heterochromatin Protein 1β (HP1β) has
890 distinct functions and distinct nuclear distribution in pluripotent versus differentiated cells. Genome
891 Biol *16*.

892 Mirabella, A.C., Foster, B.M., and Bartke, T. (2016). Chromatin deregulation in disease. Chromosoma
893 *125*, 75–93.

894 Nishibuchi, G., and Nakayama, J. (2014). Biochemical and structural properties of heterochromatin
895 protein 1: understanding its role in chromatin assembly. J. Biochem. *156*, 11–20.

896 O'Geen, H., Squazzo, S.L., Iyengar, S., Blahnik, K., Rinn, J.L., Chang, H.Y., Green, R., and Farnham, P.J.
897 (2007). Genome-wide analysis of KAP1 binding suggests autoregulation of KRAB-ZNFs. PLoS Genet. *3*,
898 e89.

899 Paik, Y.-H., Kim, J., Aoyama, T., De Minicis, S., Bataller, R., and Brenner, D.A. (2014). Role of NADPH
900 oxidases in liver fibrosis. Antioxid. Redox Signal. *20*, 2854–2872.

901 Park, J.W., Reed, J.R., Brignac-Huber, L.M., and Backes, W.L. (2014). Cytochrome P450 system
902 proteins reside in different regions of the endoplasmic reticulum. Biochem. J. *464*, 241–249.

903 Piacentini, L., Fanti, L., Negri, R., Del Vescovo, V., Fatica, A., Altieri, F., and Pimpinelli, S. (2009).
904 Heterochromatin protein 1 (HP1a) positively regulates euchromatic gene expression through RNA
905 transcript association and interaction with hnRNPs in Drosophila. PLoS Genet. *5*, e1000670.

906 Pogribny, I.P., Ross, S.A., Tryndyak, V.P., Pogribna, M., Poirier, L.A., and Karpinets, T.V. (2006).
907 Histone H3 lysine 9 and H4 lysine 20 trimethylation and the expression of Suv4-20h2 and Suv-39h1
908 histone methyltransferases in hepatocarcinogenesis induced by methyl deficiency in rats.
909 Carcinogenesis *27*, 1180–1186.

910 Postic, C., Shiota, M., Niswender, K.D., Jetton, T.L., Chen, Y., Moates, J.M., Shelton, K.D., Lindner, J.,
911 Cherrington, A.D., and Magnuson, M.A. (1999). Dual roles for glucokinase in glucose homeostasis as
912 determined by liver and pancreatic beta cell-specific gene knock-outs using Cre recombinase. J. Biol.
913 Chem. *274*, 305–315.

914 Prakash, K., and Fournier, D. (2018). Evidence for the implication of the histone code in building the
915 genome structure. BioSystems *164*, 49–59.

916 Scarfò, I., Pellegrino, E., Mereu, E., Inghirami, G., and Piva, R. (2016). Transposable elements: The
917 enemies within. Experimental Hematology *44*, 913–916.

918 Schott, S., Coustham, V., Simonet, T., Bedet, C., and Palladino, F. (2006). Unique and redundant
919 functions of C. elegans HP1 proteins in post-embryonic development. Dev. Biol. *298*, 176–187.

920 Shi, S., Larson, K., Guo, D., Lim, S.J., Dutta, P., Yan, S.-J., and Li, W.X. (2008). Drosophila STAT is
921 required for directly maintaining HP1 localization and heterochromatin stability. Nat. Cell Biol. *10*,
922 489–496.

923 Si-Tayeb, K., Lemaigre, F.P., and Duncan, S.A. (2010). Organogenesis and development of the liver.
924 Dev. Cell *18*, 175–189.

925 Strick-Marchand, H., and Weiss, M.C. (2002). Inducible differentiation and morphogenesis of
926 bipotential liver cell lines from wild-type mouse embryos. Hepatology *36*, 794–804.

927 Takaki, A., and Yamamoto, K. (2015). Control of oxidative stress in hepatocellular carcinoma: Helpful
928 or harmful? World J Hepatol *7*, 968–979.

929 Thompson, P.J., Macfarlan, T.S., and Lorincz, M.C. (2016). Long Terminal Repeats: From Parasitic
930 Elements to Building Blocks of the Transcriptional Regulatory Repertoire. Mol. Cell *62*, 766–776.

931 Vad-Nielsen, J., and Nielsen, A.L. (2015). Beyond the histone tale: HP1α deregulation in breast cancer
932 epigenetics. Cancer Biology & Therapy *16*, 189–200.

933 Vakoc, C.R., Mandat, S.A., Olenchock, B.A., and Blobel, G.A. (2005). Histone H3 lysine 9 methylation
934 and HP1gamma are associated with transcription elongation through mammalian chromatin. Mol.
935 Cell *19*, 381–391.

936 Velazquez Camacho, O., Galan, C., Swist-Rosowska, K., Ching, R., Gamalinda, M., Karabiber, F., De La
937 Rosa-Velazquez, I., Engist, B., Koschorz, B., Shukeir, N., et al. (2017). Major satellite repeat RNA
938 stabilize heterochromatin retention of Suv39h enzymes by RNA-nucleosome association and
939 RNA:DNA hybrid formation. Elife *6*.

940 Weisend, C.M., Kundert, J.A., Suvorova, E.S., Prigge, J.R., and Schmidt, E.E. (2009). Cre activity in fetal
941 albCre mouse hepatocytes: Utility for developmental studies. Genesis *47*, 789–792.

942 Wolf, G., Yang, P., Füchtbauer, A.C., Füchtbauer, E.-M., Silva, A.M., Park, C., Wu, W., Nielsen, A.L.,
943 Pedersen, F.S., and Macfarlan, T.S. (2015). The KRAB zinc finger protein ZFP809 is required to initiate
944 epigenetic silencing of endogenous retroviruses. Genes Dev. *29*, 538–554.

945 Yang, P., Wang, Y., and Macfarlan, T.S. (2017). The Role of KRAB-ZFPs in Transposable Element
946 Repression and Mammalian Evolution. Trends Genet. *33*, 871–881.

947

948

949

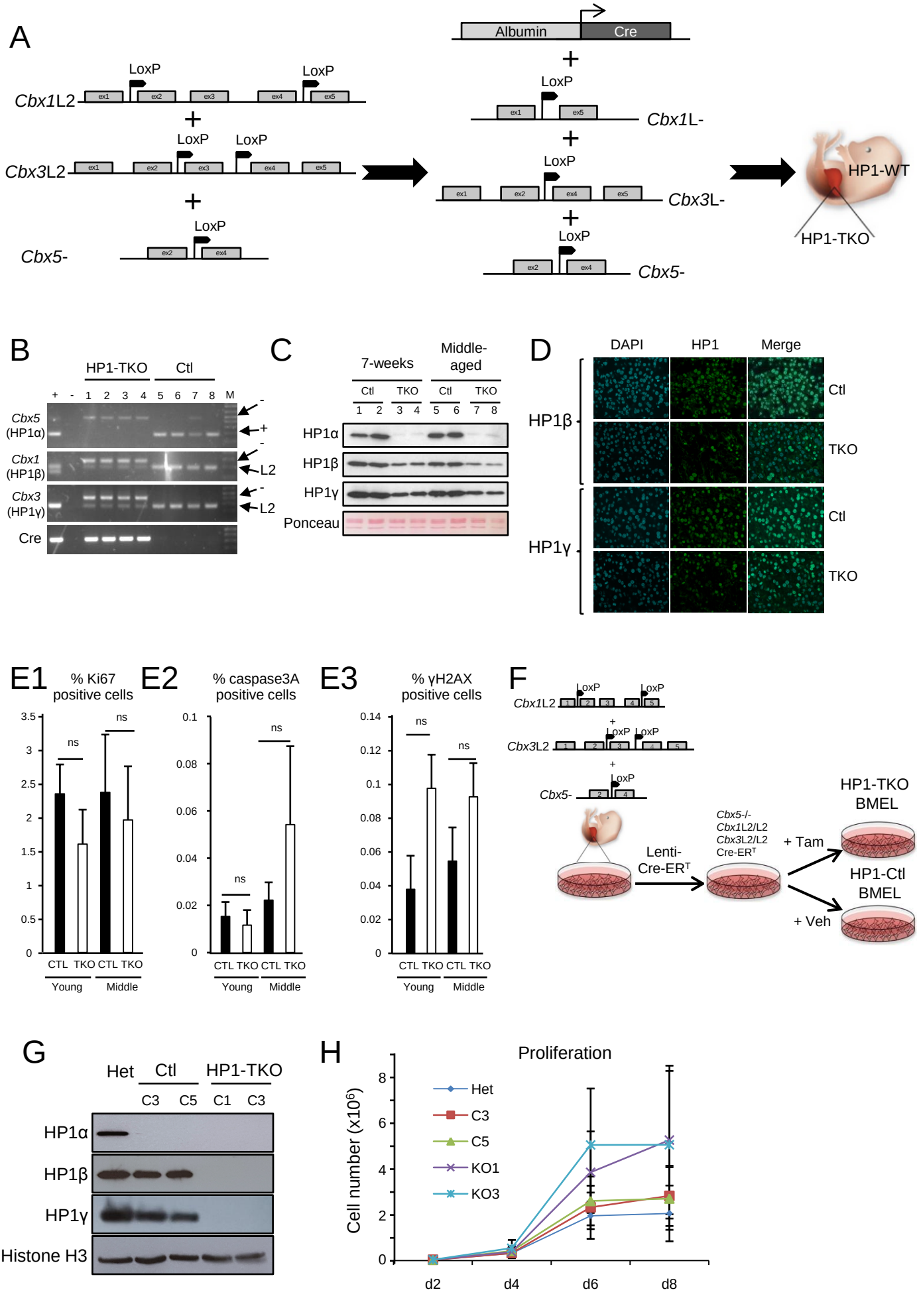

Figure 1. Saksouk & Hajdari et al.

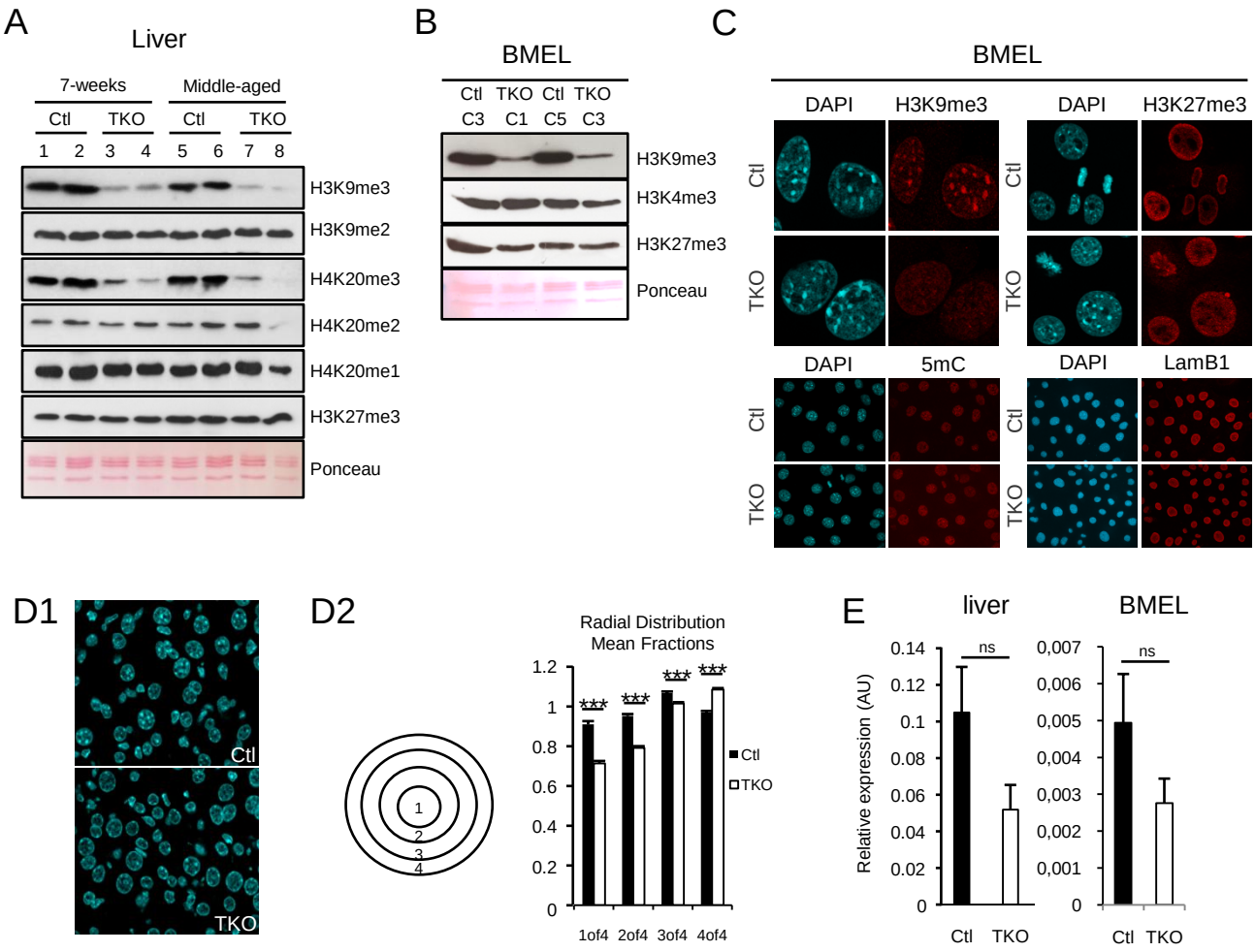

Figure 2 Saksouk & Hajdari et al,

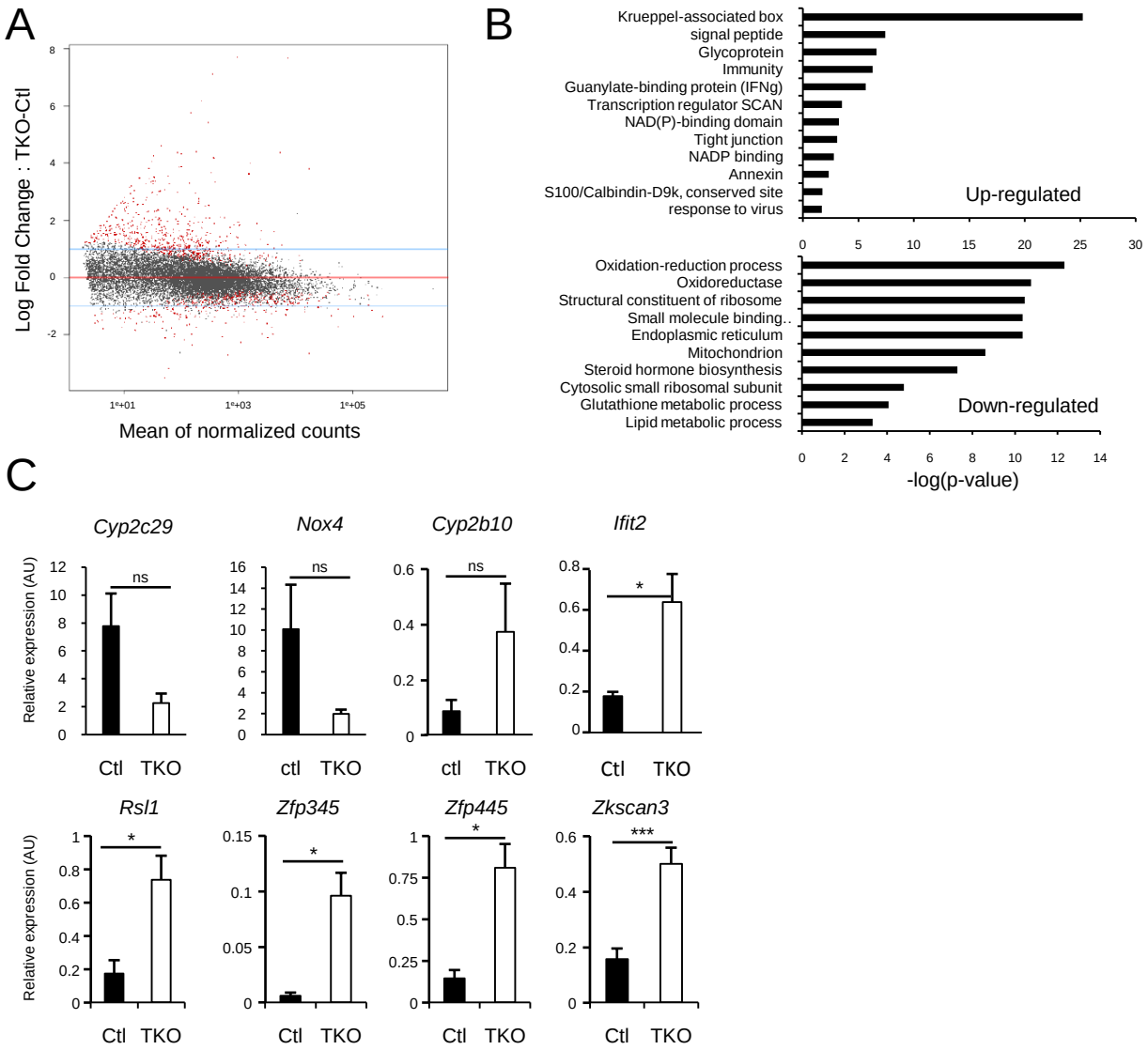

Figure 3 Saksouk & Hajdari et al,

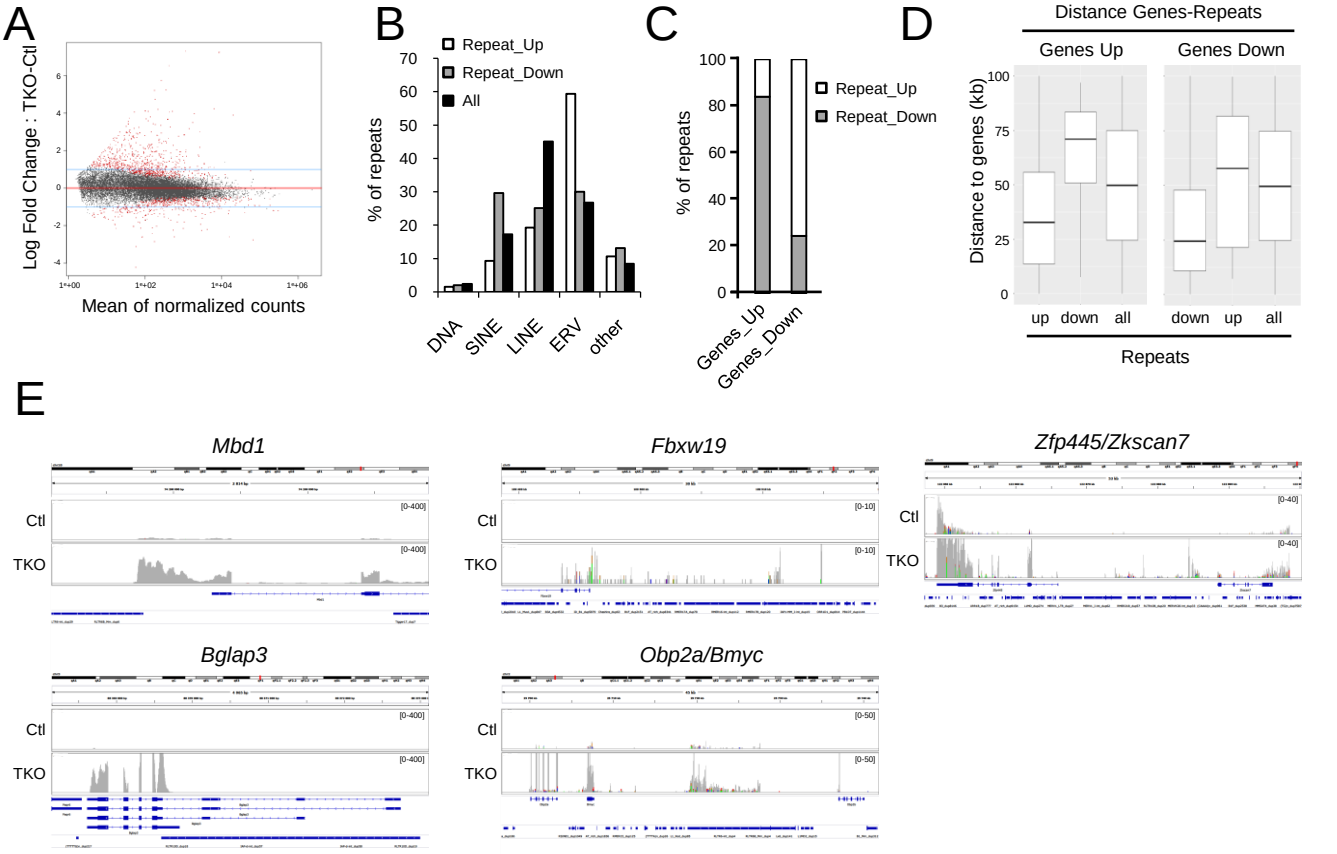

Figure 4 Saksouk & Hajdari et al,

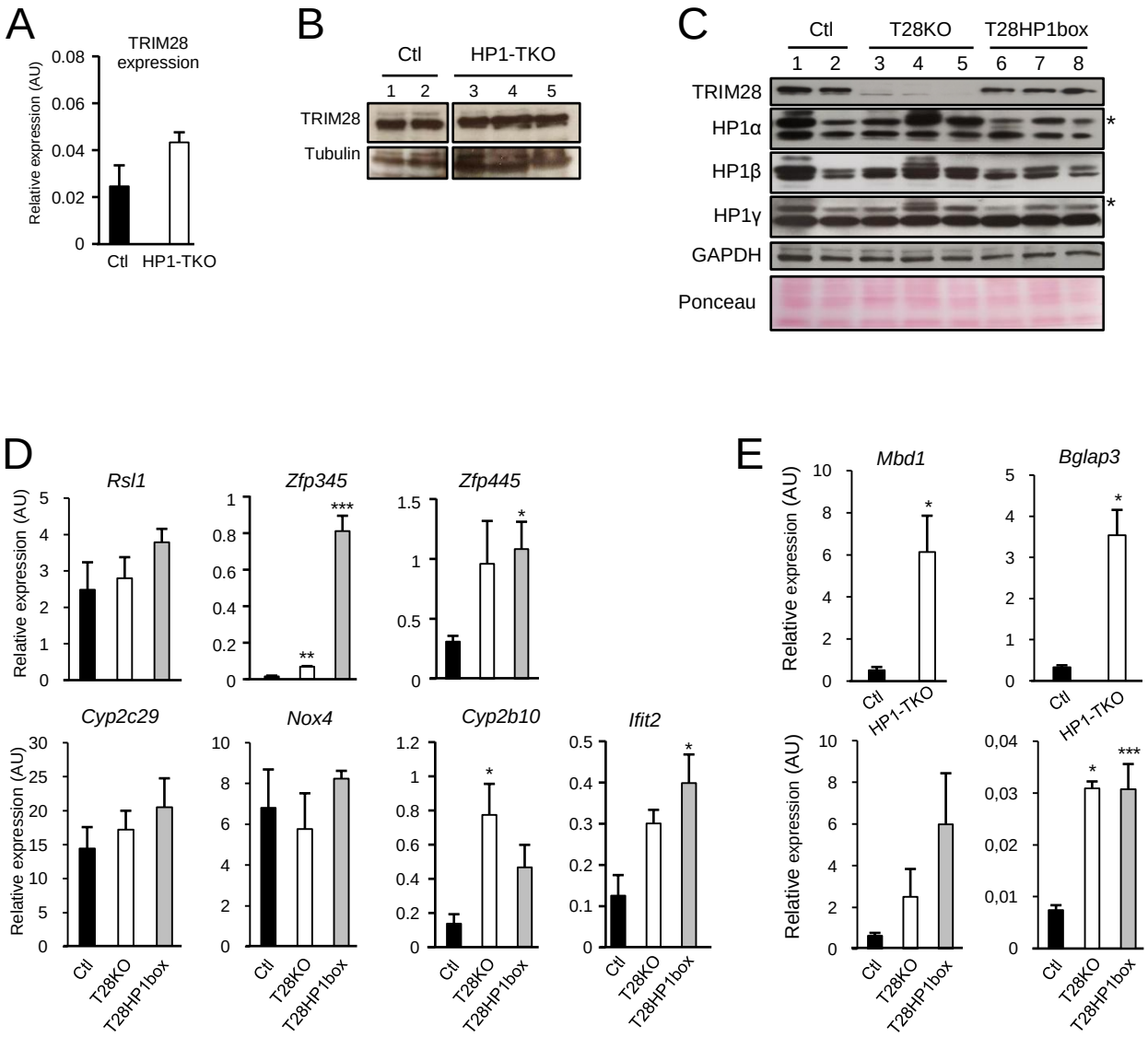

Figure 5, Saksouk & Hajdari et al,

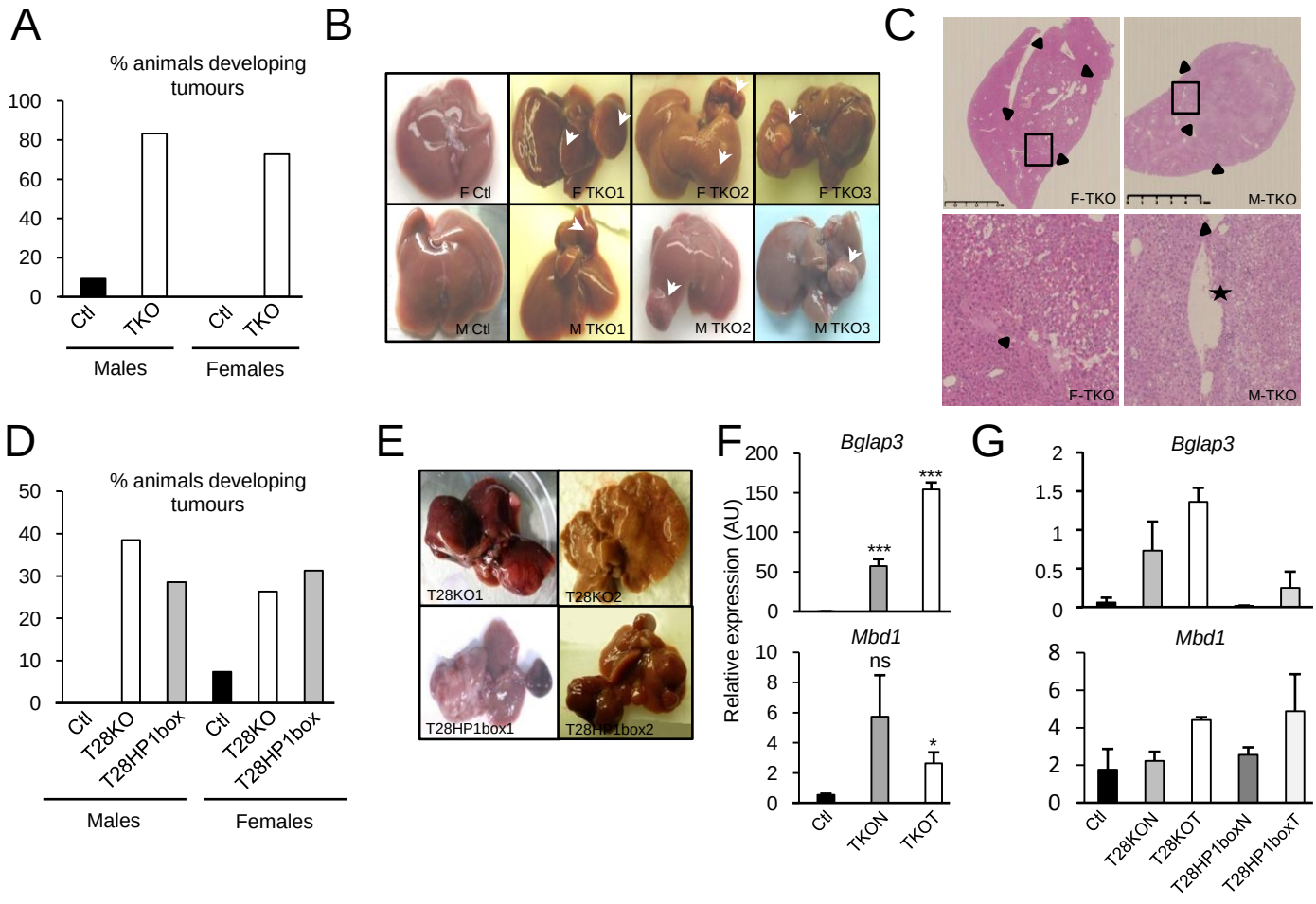

Figure 6 Saksouk & Hajdari et al,

Table 1: HP1-dependent p450 genes.

Gene name	Log2 fold-change	padj	Redox	Endoplasmic reticulum	Drug metabolism	Lipid metabolism	Steroid synthesis
Cyp2b10	4.06	1.41E-38	1	1	0	0	1
Cyp2b9	2.68	4.51E-10	1	1	0	0	1
Cyp2b13	1.80	0.000120	0	0	0	0	1
Cyp4f16	1.63	1.36E-09	0	0	0	0	0
Cyp2d12	1.38	0.000468	0	0	0	0	1
Cyp2a4	1.09	0.0342	0	0	0	0	0
Cyp2a22	1.06	0.000559	0	0	0	0	0
Cyp2f2	-0.65	0.00318	1	1	0	0	0
Cyp4f13	-0.67	0.0151	0	0	0	0	0
Cyp2r1	-0.72	0.0173	1	1	0	0	0
Cyp27a1	-0.83	1.30E-05	1	0	0	0	0
Cyp2d37-ps	-0.83	0.0319	0	0	0	0	0
Cyp3a25	-0.85	0.00222	1	1	0	0	1
Cyp39a1	-0.88	0.00164	1	1	0	1	0
Cyp2e1	-0.94	7.81E-05	1	1	1	0	1
Cyp2d26	-0.95	2.57E-05	1	1	0	0	1
Cyp2a5	-0.97	0.00129	0	0	0	0	0
Cyp2d13	-1.00	0.00445	0	0	0	0	0
Cyp1a2	-1.25	3.65E-12	1	1	1	1	1
Cyp2c53-ps	-1.31	0.01178	0	0	0	0	0
Cyp2d40	-1.42	6.83E-06	0	0	0	0	1
Cyp46a1	-1.64	0.000629	1	1	0	1	0
Cyp3a59	-2.15	3.62E-17	1	0	0	0	0
Cyp2c44	-2.20	2.18E-20	0	0	0	0	1
Cyp2c29	-2.60	7.65E-25	1	1	0	0	1

(1) found and (0) not found according to the David Gene Ontology software.